International Journal of GEOMATE, Sept. 2022, Vol.23, Issue 97, pp.188-195
ISSN: 2186-2982 (P), 2186-2990 (O), Japan, DOI: https://doi.org/10.21660/2022.97.3483
Geotechnique, Construction Materials, and Environment

CONTRIBUTION OF STEEL FIBERS ON DUCTILITY OF CONFINED CONCRETE COLUMNS

Agoes Soehardjono[1], *Bambang Sabariman[2,3], Wisnumurti[1], and Ari Wibowo[1]

[1]Department of Civil Engineering, Universitas Brawijaya, Indonesia
[2]Department of Civil Engineering, Universitas Negeri Surabaya, Indonesia
[3]Doctoral Candidate, Department of Civil Engineering, Universitas Brawijaya, Indonesia

*Corresponding Author, Received: 21 June 2022, Revised: 09 July 2022, Accepted: 02 August 2022

ABSTRACT: Displacement and curvature ductilities are the key parameters in the design of structural columns because columns are very important structural members for the strength and resilience of a building. To increase column ductility, one common approach is by providing confinement. The number of reinforcing bars and its confitheiration commonly became the main parameters studied by researchers. The outcomes showed that columns were able to reach high lea vel of ductility (μ_Δ>6) by using heavy transverse reinforcement and specific detailing. Another approach to improve the column ductility is by applying steel fiber to the concrete to increase the stress and the strain behavior of concrete. These two approaches are combined and studied in the experimental tests presented in this paper. The confinement and fiber used in the reinforced concrete specimens were square stirrups and steel fiber with volumetric ratio V_f ranging 0-2%. from All columns were subjected to quasi-cyclic horizontal load at the column top until reaching failure at about at $0.80P_{h\text{-}max}$. An axial load of P_a about 12% axial load capacity is maintained throughout the test. This study indicated that fiber could contribute to extend the inelastic displacement of the column so that the specimen can reach a high ductile displacement ductility, especially in columns with a ratio of V_f=1%.

Keywords: Ductility, Inelastic, Quasi-cyclic, Steel fiber.

1. INTRODUCTION

The use of reinforcement in concrete has been known to improve the strength and ductility of the concrete members [1]. Reinforcement plays a very important role in concrete members [2]. Several researchers have carried out the need to increase displacement and curvature ductilities [3-9]. On the other hand, in research that seeks to increase the stress-strain in concrete, some of these researchers have attempted in various ways [10-11], including by applying reinforcement using steel fiber to the unconfined concrete members [12-16] and some to the confined concrete members [17-19] the results of this study indicate an increase in the stress-strain of concrete due to the use of steel fiber.

Currently, fiber is widely applied to various concrete members, because in general, it can improve the performance of concrete. Steel fiber is one of the most widely used fibers in both research and practice. These fibers have the potential to increase the tensile strength of concrete [20], as well as increase the flexural strength of concrete [21]. In addition, steel fiber is superior in crack propagation resistance and provides increased post-crack ductility due to its brittleness [22-24], it can even increase failure load [25] by 20 percent, increase stiffness by 3.4-11 times during loading and increase crack resistance about 2.6 times.

This research combines the application of confinement and steel fiber to reinforced concrete columns. It is expected that there is an increase in displacement ductility and curvature ductility of reinforced concrete columns.

2. RESEARCH SIGNIFICANCE

This study conducted a study to determine the contribution of steel fiber applied to confined concrete columns. The contribution in question is how the influence of steel fiber on the terms of displacement ductility and curvature ductility of reinforced concrete columns. Given these conditions, this study seeks to increase the ductility of the column by adding steel fiber.

3. MATERIALS

Some of the materials and methods used in this research are as follows:

3.1 Materials

The use of materials in the study included the use of steel fiber, stirrups, main reinforcement, and normal concrete. All of the column sizes in the study were 200x200 mm and the test area height was 800 mm. Determination of the size of the column test area has followed the requirements of the failure mechanism of the test object [26]. Column restraints are designed based on the value of the Z_m confinement [27]. The direction of the main anchorage has been adjusted to the quasi-cyclic loading pattern, directed out of the column area [28], this aims to avoid failure of the main reinforcement of the column during the quasi-cyclic test.

The number of steel fibers, stirrups, main reinforcement, and normal concrete was designed based on several manufacturers' products, previous research, and existing regulations in Indonesia [29], this rule adopts the ACI 318M-14 rule. The descriptions of several materials and the results of the material tests used in this study are as follows:

Fig.1 Steel fiber 3D, material properties: E=210,000 N/mm^2, l=60 mm, d=0.75 mm, aspect ratio (l/d)=80

Table 1 Specifications of D8 steel bar for transverse reinforcement (stirrup)

Specimen	f'$_y$ (MPa)	Elongation (%)
D8.1	543.57	24.42
D8.2	525.88	27.93
D8.3	571.04	22.29
Average	546.83	24.88

Table 2 Specifications of D13 steel bar for longitudinal reinforcement

Specimen	f'$_y$ (MPa)	Elongation (%)
D13.1	418.87	23.82
D13.2	381.64	36.68
D13.3	417.12	20.54
Average	405.88	27.01

Table 3 Mix design

Material	Unit weight (kN/m^3)
Cement	4.30
Water	1.90
Coarse Agg. (10-20) mm	9.78
Sand	8.00
Admixture Type D	0.01
Admixture Type F	0.03
Total solid/volume	24.02

Table 4 Concrete cylinder compression test results

Specimen	f'c (MPa)
Cylinder$_1$	27.80
Cylinder$_2$	26.45
Cylinder$_3$	26.77
Average	27.01

Based on the tables above, the value of the Z_m confinement is calculated.

Table 5 Details of column test specimens

Specimen	Longitudinal reinforcement	Stirrups	V_f	Z_m
$C_{50.0}$	8D13	D8-50	0	19.63
$C_{50.1}$	8D13	D8-50	1%	19.63
$C_{50.2}$	8D13	D8-50	2%	19.63

Note V_f =Volumetric steel fiber, ρ_l = 2.65%

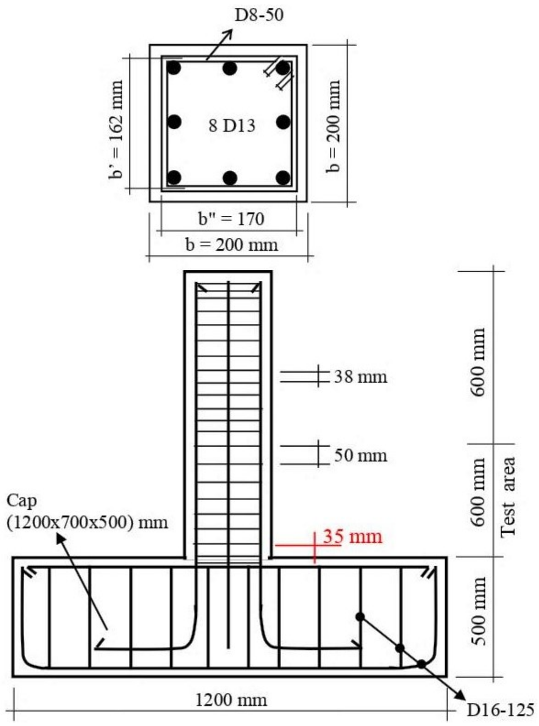

Fig.2 Column reinforcement

3.2. Yield Displacement

The displacement point at first yielding can be measured based on the measurement results from the strain gauge attached to the main reinforcement, but some researchers practically define the point based on Figure 3. Determination of the melting point of the first displacement Δ_y by drawing a horizontal line $0.75P_{h\text{-}max}$ to the right tangent to the envelope curve to get Point a. Then draw a straight line oa meets the horizontal line $P_{h\text{-}max}$ to get point b, after that draw a vertical line down, the value of Δ_y is obtained.

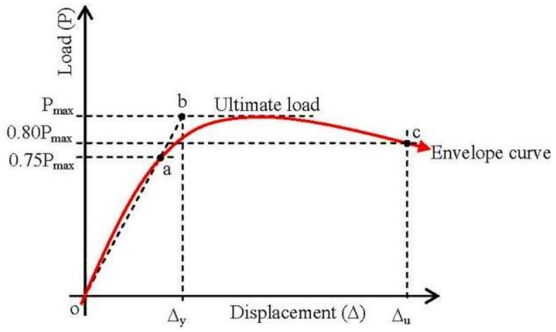

Fig.3 Definition of yield displacement [30-32]

Meanwhile, the ultimate displacement value is based on a 20% decrease in strength, namely $0.80P_{h\text{-}max}$. By drawing a line from $0.80P_{h\text{-}max}$ to the right and touching the envelope curve line, you will find point b, from point b then a vertical line will be drawn down to get the ultimate displacement value Δ_u.

3.3. Displacement Ductility and Curvature Ductility

The displacement ductility value is obtained based on the following calculation:

$$\mu_\Delta = \frac{\Delta_u}{\Delta_y} \tag{1}$$

Some researchers make criteria for displacement ductility as follows [33-34]:

Very ductile : $\mu_\Delta>6$
Moderate ductility : $4<\mu_\Delta\leq 6$
Limited ductility : $2<\mu_\Delta\leq 4$
Brittle : $\mu_\Delta\leq 2$

Meanwhile, the determination of the curvature at the first yielding and the ultimate curvature is almost the same as the determination of the melting point of the first displacement Δ_y. For that, some researchers also practically determine it as shown below.

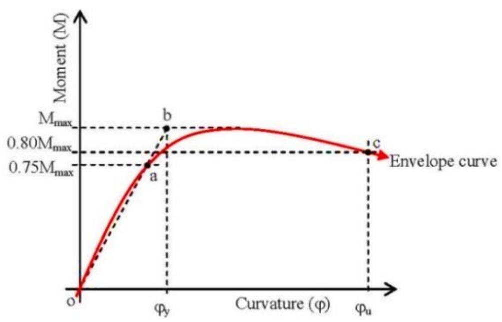

Fig.4 Definition of Curvature [30-32]

Based on Fig. 5 can be calculated the value of curvature (φ). While the value of curvature ductility is obtained based on Fig. 4, the value is calculated as follows:

$$\mu_\varphi = \frac{\varphi_u}{\varphi_y} \tag{2}$$

Some researchers make the criteria of curvature ductility as follows [35]:

Very ductile : $\mu_\varphi>16$
Moderate ductility : $8\leq\mu_\varphi\leq 16$
Limited ductility : $8<\mu_\varphi$

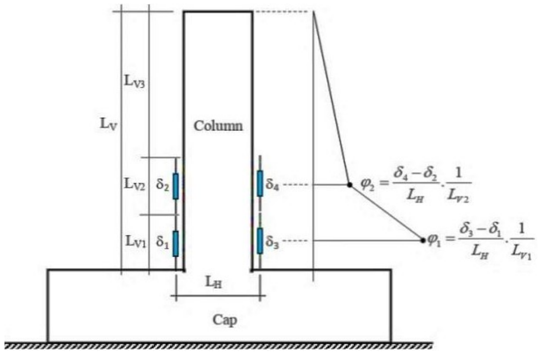

$$\varphi_2 = \frac{\delta_4-\delta_2}{L_H}\cdot\frac{1}{L_{V2}}$$
$$\varphi_1 = \frac{\delta_3-\delta_1}{L_H}\cdot\frac{1}{L_{V1}}$$

Fig.5 Determination of curvature [36]

Figure 5 shows the calculation of column curvature, namely φ_1 and φ_2. This calculation is based on the change in shortening and elongation of the left-right side of the column due to a load of P_h. These changes are recorded by the LVDT mounted on the left-right side of the column.

4. METHODS

All columns were tested quasi-cyclically where the drift test was following ACI 374.1-05. The alternating cycle was performed 3 times each, starting with a 0.2% drift. The next drift was carried out with a 1.25<drift≤1.5 patterns from the previous drift. The column test is stopped if the horizontal P load has reached $0.80P_{h\text{-}max}$ or during the test load can no longer be added, this of course occurs at drifts exceeding 3.5%. The drift plan of this cyclic column test is shown in Fig.6 and Table 6.

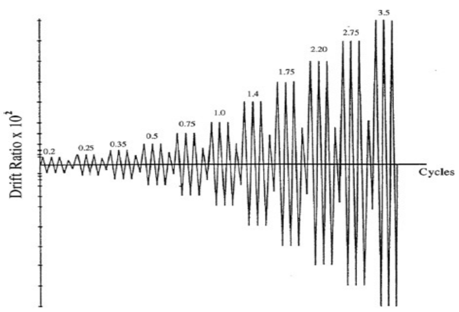

Fig.6 Loading cycle with displacement control according to ACI 374.1-05 [37]

Table 6 Drift-control tests of each column specimen, h column 800 mm.

Cycle #	Drift (%)	Displacement (mm)
1	0.20	1.60
2	0.25	2.00
3	0.35	2.80
4	0.50	4.00
5	0.75	6.00
6	1.00	8.00
7	1.40	11.20
8	1.75	14.00
9	2.20	17.60
10	2.75	22.00
11	3.50	28.00
12	4.38	35.00
13	5.47	43.75
14	6.84	54.69
15	8.54	68.36
16	10.68	85.45

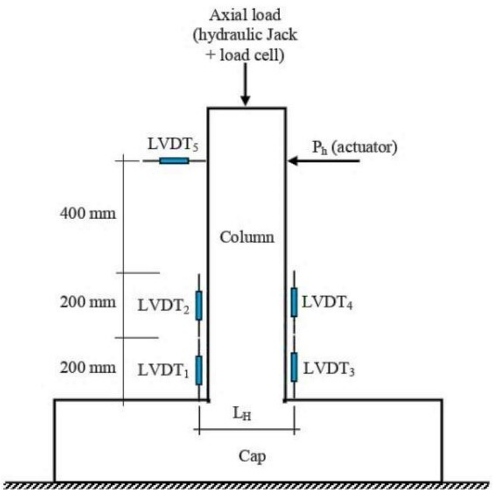

Fig.7 Schematic of test setup of the specimen
Note: LVDT = Linear Variable Displacement Transducer

Fig.8 Collapsed condition of the column

Schematic Figure 7 is made to represent the test specimen setup, and some of the tools used to obtain measurement data as input for calculating displacement ductility and curvature ductility.

While Fig.8 shows the actual setup of the column test. It shows that the column has been in a collapsed condition, where after the $P_{h\text{-comp}}$ loading was carried out in a certain cycle, the Ph-comp load was released, and the column remained tilted. To be able to return to its original position, the column must be subjected to a $P_{h\text{-tension}}$ load.

5. RESULT AND DISCUSSION

The testing process was carried out according to the plan above. Data recording is obtained simultaneously on several installed devices as shown in the test setup. The results of the simultaneous data recording are recorded on a universal recorder in the form of changes in LVDT short height, LVDT displacement, and the amount of P_h. The application of P_{axial} was maintained constant at 0.12f'cAg or equivalent to 10 kN while the administration of P_h starting from 0 kN to exceeding the $P_{h\text{-max}}$ was attempted to achieve a decrease of 20% from the $P_{h\text{-max}}$. The test results are detailed as follows.

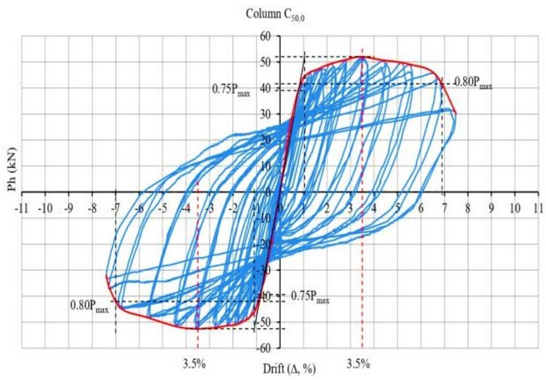

Fig.9 Envelope drift hysteresis column $C_{50.0}$

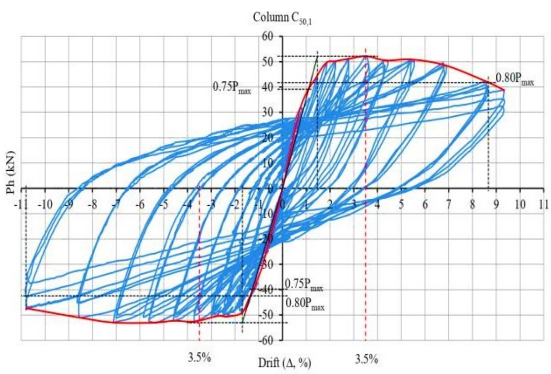

Fig.10 Envelope drift hysteresis column $C_{50.1}$

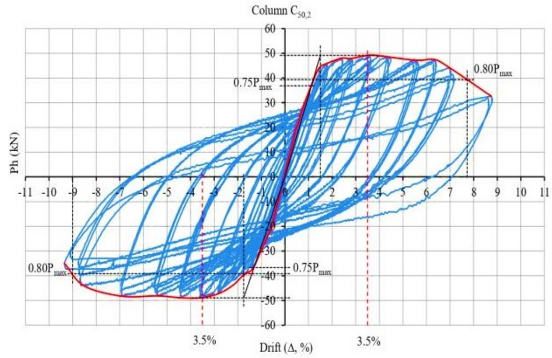

Fig.11 Envelope drift hysteresis column $C_{50.2}$

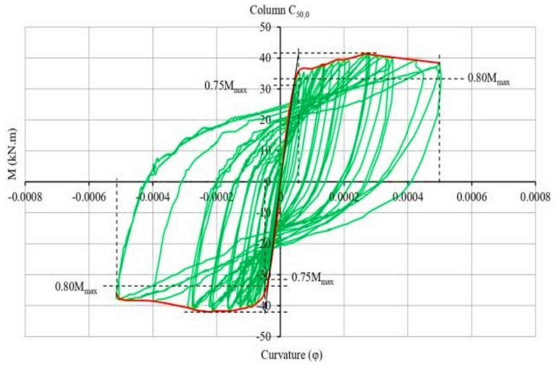

Fig.12 Envelope curvature hysteresis column $C_{50.0}$

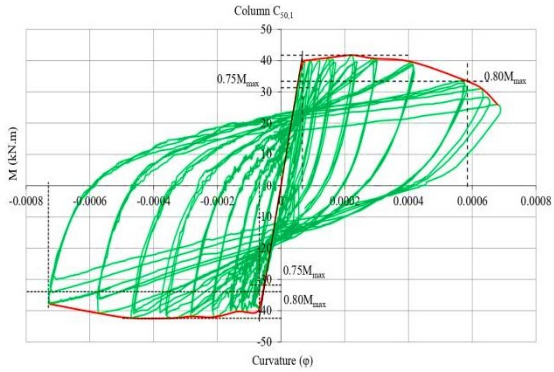

Fig.13 Envelope curvature hysteresis column $C_{50.1}$

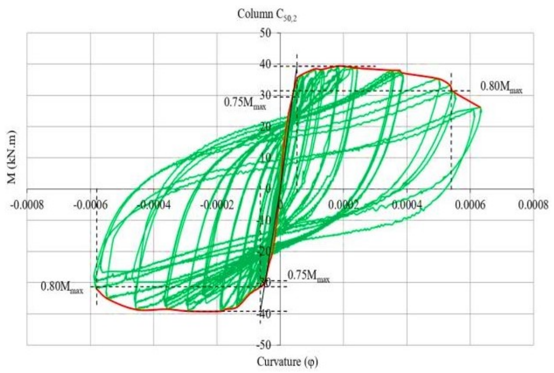

Fig.14 Envelope curvature hysteresis column $C_{50.2}$

Table 7 Displacement ductility

Column	Displacement ductility (μ_Δ)	Criteria
$C_{50.0}$	6.36	very ductile
$C_{50.1}$	6.39	very ductile
$C_{50.2}$	5.14	moderate ductile

Table 8 Curvature ductility

Column	Curvature ductility (μ_φ)	Criteria
$C_{50.0}$	10.57	moderate ductile
$C_{50.1}$	10.73	moderate ductile
$C_{50.2}$	9.20	moderate ductile

Table 9 Maximum load and deflection

Column	Maximum horizontal load		Maximum deflection (inelastic)	
	Drift	$P_{h\text{-}max}$ (kN)	$Drift_{max}$	P_h (kN)
$C_{50.0}$	28.80 mm (3.60%)	52.56	59.21 mm (7.40%)	32.16
$C_{50.1}$	43.38 mm (5.42%)	53.03	86.18 mm (10.77%)	47.38
$C_{50.2}$	28.79 mm (3.51%)	48.94	74.77 mm (9.34%)	35.01

The column crack appearance corresponds to Fig.8 or is perpendicular to the horizontal load direction as shown in Figs. 15 to 17.

Fig.15 Column crack $C_{50.0}$

Column cracks were all located in the plastic hinge area of the column. The cracks in the $C_{50.0}$ column (Fig. 15) tend to have a shear crack pattern, while the $C_{50.1}$ column cracks (Fig. 16) tend to be irregular but there is still a lot of rubble from the concrete cracks attached to the plastic hinge area. The sticking of this rubble was due to the bond between the concrete rubble and the steel fiber with V_f = 1%. While in Fig. 17, the column using V_f=2% shows that only a few cracks occurred. The least of these cracks were due to the decrease in the strength of the $C_{50.2}$ column.

Fig.16 Column crack $C_{50.1}$

Fig.17 Column crack $C_{50.2}$

The focus of this research was to observe the contribution of steel fiber to column ductility, both displacement ductility, and curvature ductility. Figures 9-14 and Tables 7-8 show the behavior of the column in this study, where the column is given a constant axial compression force and a horizontal force until it collapses, the failure has exceeded $0.80P_{h\text{-}max}$, where the $0.80P_{h\text{-}max}$ limit is an acceptable capability limit of a column under cyclic loading.

The effect of spiral reinforcement and square stirrup reinforcement combined with steel fiber has been shown to increase the stress-strain capacity of concrete [17-19]. In this study, it was seen that there was an increase in the capacity of the $P_{h\text{-}max}$ force due to the influence of the restraints and steel fiber and all of the $P_{h\text{-}max}$ occurred at around 3.5% drift. According to SNI 2847:2019 (ACI 318-14), it is explained that the column test must produce a column that can reach a drift of 3% without experiencing a drastic decrease in strength. This means that the columns $C_{50,0}$, $C_{50,1,}$ and $C_{50,2}$ are all able to exceed these rules.

The purpose of SNI 2847:2019 (ACI M318-14) is that at $0.80P_{h\text{-}max}$ or a 20% decrease in column strength occurs, the column must be able to deform at a 3% drift, but in this study an increase in peak load up to drift 5.42% new decrease in strength.

The results of observations on displacement ductility, columns $C_{50.0}$ and $C_{50.1}$ are sufficient because they have reached a displacement ductility of μ_Δ>6 (very ductile). While $C_{50.2}$ has only reached moderate ductility, this is due to V_f>1% which disrupts aggregate interlocking due to too much steel fiber, which also reduces column capacity.

In observation of the curvature ductility, all test objects are still included in the moderate ductility criteria. This is because the stirrups used are only two-legged with Z_m=19.631, to increase it can be done by reducing the value of Z_m<19.631 by increasing the number of stirrup legs, the smaller the Z_m value, the better the concrete restraint.

In this study (Table 9), the $P_{h\text{-}max}$ $C_{50.1}$ was at a drift of 5.42%, and the drift$_{max}$ $C_{50.1}$ occurred at a drift of 10.77% at $P_{h\text{-}inelastic}$=47.38 kN, while the drift$_{max}$ $C_{50.2}$ occurred at a drift of 9.34%. All of them are bigger than $P_{h\text{-}max}$ and drift$_{max}$ $C_{50.0}$.

6. CONCLUSION

Based on the results above, it can be seen that the displacement ductility of all columns has entered the very ductile criteria, while the curvature ductility of all columns in this study is still in a moderately ductile position. However, it can be seen that steel fiber has contributed to the column ductility and has contributed to extending the displacement at $0.80P_{h\text{-}max}$, especially in columns with a ratio of V_f =1%.

7. ACKNOWLEDGMENTS

The authors gratefully acknowledge PT. Wijaya Karya Beton Tbk. Jakarta Indonesia, which has assisted in the implementation of this research and also the research scholarship assistance scheme for the doctoral program.

8. REFERENCES

[1] Raka I G. P., Tavio, and Astawa M. D., State-of-the-Art Report on Partially-Prestressed

Concrete Earthquake-Resistant Building Structures for Highly-Seismic Region, Procedia Engineering, Vol. 95, 2014, pp. 43-53.
[2] Tavio, Anggraini R., Raka I G. P., and Agustiar, Tensile Strength/Yield Strength (TS/YS) Ratios of High-Strength Steel (HSS) Reinforcing Bars, AIP Conference Proceedings, Vol. 1964, No. 1, 2018, pp. 020036-1–020036-8.
[3] Park R., and Paulay T., Reinforced Concrete Structures, John Willey & Sons, Inc., New York, 1975.
[4] Paulay T., and Priestley M.J.N., Seismic Design of Reinforced Concrete and Masonry Building, John Willey & Sons, Inc., New York, 1992.
[5] Machmoed S. P., Tavio and Raka I G. P., Performance of Square Reinforced Concrete Columns Confined With Innovative Confining System Under Axial Compression, International Journal of GEOMATE, Vol.21, Issue 85, 2021, pp. 137-144.
[6] Seong D. J., Kim T. H., Oh M. S., and Shin H. M., Inelastic Performance of High-Strength Concrete Bridge Columns under Earthquake Loads. Journal of Advanced Concrete Technology Vol. 9, No. 2, 2011, pp. 205-220.
[7] Pudjisuryadi P., and Tavio, Performance of Square Reinforced Concrete Columns Externally Confined by Steel Angle Collars under Combined Axial and Lateral Load, Procedia Engineering, Vol. 125, 2015. pp. 1043–1049.
[8] Tavio, and Kusuma B., Ductility of Confined Reinforced Concrete Columns with Welded Reinforcement Grids, Excellence in Concrete Construction through Innovation-Proceedings of the International Conference on Concrete Construction, 2009, pp. 339-344,
[9] Tavio, and Kusuma B., Strength and Ductility Enhancement of Reinforced HSC Columns Confined with High-Strength Transverse Steel, Proceedings of the Eleventh East Asia-Pacific Conference on Structural Engineering and Construction (EASEC-11), 2008, pp. 350-351.
[10] Tavio, and Kusuma B., Investigation of Stress-Strain Models for Confinement of Concrete by Welded Wire Fabric, Procedia Engineering, Vol. 14, 2011, pp. 2031–2038.
[11] Tavio, and Kusuma B., Stress-Strain Model for High-Strength Concrete Confined by Welded Wire Fabric, Journal of Materials in Civil Engineering, Vol. 21, No. 1, 2009, pp. 40–45.
[12] Ezeldin A. S., and Balaguru P. N., Normal and High-Strength Fiber Reinforced Concrete under Compression, J. Mater. Civ. Eng., 4(4), 1992, pp. 415-429.
[13] Nataraja M. C., Dhang N., and Gupta A. P., Stress-Strain Curve for Steel-Fiber Reinforced Concrete under Compression, Cem. Concr. Compos., 21, 1999, pp. 383-390.
[14] Dhakal R. P., Wang, C., and Mander J. B., Behavior of Steel Fibre Reinforced Concrete in Compression, UC Research Repository, University Library, University of Canterbury, http://hdl.handle.net/10092/4408, 2017.
[15] Hassouna F. M. A., and Jung Y. W., Developing a Higher Performance and Less Thickness Concrete Pavement: Using a Nonconventional Concrete Mixture, Hindawi, Advances in Civil Engineering, Volume 2020, Article ID 8822994, 2020, 8 pages.
[16] Junior O., et al., Stress-strain curves for Steel Fiber-Reinforced Concrete in Compression, Revista Materia Vol 15 No 2, 2010, pp. 260-266.
[17] Sabariman B., Soehardjono A., Wisnumurti, Wibowo A., and Tavio, Stress-Strain Model for Confined Fiber-Reinforced Concrete under Axial Compression, Archives of Civil Engineering, Vol. 66, No. 2, 2020, pp. 119-133.
[18] Sabariman B., Soehardjono A., Wisnumurti, Wibowo A., and Tavio, Stress-Strain Behavior of Steel Fiber-Reinforced Concrete Cylinders Spirally Confined with Steel Bars, Advances in Civil Engineering, 2018, pp. 1-8.
[19] Lejano B. A., Evaluation of Different Fiber Reinforced Mortar as Retrofitting Materials for RC Columns, International Journal of GEOMATE, Vol.13, Issue 35, 2017, pp. 40-47.
[20] Solahuddin B. A., Strengthening of Reinforced Concrete with Steel Fibre: A Review, Materials Science Forum, Volume 1056, https://doi.org/10.4028/p-3g0h57, 2022, pp. 81-86.
[21] Saloma and Sulthan F., Influence of Hooked-End Steel Fibers on Flexural Behavior of Steel Fiber Reinforced Self-Compacting Concrete (SFRSCC), International Journal of GEOMATE, Vol.23, Issue 95, https://doi.org/10.21660/2022.95.3310, 2022, pp. 127-135.
[22] Chanh N. V., , Steel fiber reinforced concrete, 8-Joint Vietnam Joint Seminars, Ho Chi Minh City University of Technology, https://www.jsce.or.jp/committee/concrete/e/newsletter/newsletter05/8-Vietnam%20Joint%20Seminar(CHANH).pdf, pp. 108-116.
[23] Behbahani H. P., et al., Flexural Behavior of Steel-Fiber-added-RC (SFARC) Beams with C30 and C50 Classes of Concrete, International Journal of Sustainable Construction Engineering & Technology, Vol. 3, Issue 1, 2012, pp. 54-64.

[24] Andriichuk O., Babich V., Yasyuk I., and Uzhehov S., The Impact of The Reinforcement Percentage On The Stress-Strain State Of The Bending Steel Fiber Reinforced Concrete Elements, MATEC Web of Conferences 230, https://doi.org/10.1051/matecconf/201823002001, 2018, pp. 1-5.

[25] Oleg R., and Linar S., Reinforced Concrete Beams Strengthened with Steel Fiber Concrete, IOP Conf. Series: Materials Science and Engineering 890 STCCE-2020, doi:10.1088/1757-899X/890/1/012045, 2020, pp. 1-11.

[26] ASCE/SEI 41-0.6, Seismic Rehabilitation of Existing Buildings, ASCE, The USA, 2007.

[27] Scott B. D., Park R., and Priestley, M. J. N., Stress-Strain Behavior of Concrete Confined by Overlapping Hoops at Low and High Strain Rates, J. American Concrete Institute, 79, 1982, pp. 13-27.

[28] Sabariman B., and Sofianto M. F., Study of crack patterns in beam-column joint due to upwards anchoring beam effect AIP Conference Proceedings 1855, http://doi.org/10.1063/1.4985500, 2017, pp. 040004.1-8

[29] Indonesian National Standard, SNI 2847:2019, Requirements of Structural Concrete for Buildings (in Indonesian), 2019.

[30] Brachmann I., Browning J. A., and Matamoros A., Drift-Dependent Confinement Requirements for Reinforced Concrete Columns Under Cyclic Loading, ACI Structural Journal, 2004, pp. 669-677.

[31] Park R., Evaluation of Ductility of Structures and Structural Assemblages From Laboratory Testing, Bulletin of The New Zealand National Society for Earthquake Engineering, Vol. 22, No.3, 1989, pp. 155-166.

[32] Park R., State-of-the-Art Report Ductility Evaluation From Laboratory and Analytical Testing, Proceedings of Ninth World Conference on Earthquake Engineering, Tokyo-Kyoto, JAPAN (Vol. VIII), 1988, pp. 605-616.

[33] Ghee A. B., Priestley M. J. N., and Paulay T., Seismic Shear Strength of Circular Reinforced Concrete Columns. ACI Structural Journal, 1989, pp. 45-59.

[34] Ghee A. B., Seismic Shear Strength of Circular Bridge Piers, A thesis submitted in partial fulfillment of the requirements for the Degree of Doctor of Philosophy in Civil Engineering at the University of Canterbury, Christchurch, New Zealand, 1985.

[35] Sheikh S. A., and Khoury S. S., A Performance-Based Approach for the Design of Confining Steel in Tied Columns, ACI Structural Journal, 1997, pp. 421-431

[36] Wibowo A., Wilson J. L., Lam N. T. K., and Gad E. F., Drift Capacity of Lightly Reinforced Concrete Columns, Australian Journal of Structural Engineering, http://dx.doi.org/10.7158/S13-002.2014.15.2, Vol. 15, No. 2, April 2014, pp. 131-150.

[37] ACI Committee 374, ACI 374.1-05 (Reapproved 2014), Acceptance Criteria for Moment Frames Based on Structural Testing and Commentary, An ACI Standard, American Concrete Institute 38800 Country Club Drive, Farmington Hills, MI 48331, USA, 2014.